

# UC Irvine

## UC Irvine Previously Published Works

### Title

Carbon flux and forest dynamics: Increased deadwood decomposition in tropical rainforest tree-fall canopy gaps

### Permalink

<https://escholarship.org/uc/item/8sk9b0k7>

### Journal

Global Change Biology, 27(8)

### ISSN

1354-1013

### Authors

Griffiths, Hannah M  
Eggleton, Paul  
Hemming-Schroeder, Nicole  
[et al.](#)

### Publication Date

2021-04-01

### DOI

10.1111/gcb.15488

Peer reviewed

1 Carbon flux and forest dynamics: increased deadwood  
2 decomposition in tropical rainforest tree-fall gaps  
3

4 **Running title:** Faster deadwood decay in canopy gaps  
5

6 **Authors:** H. M. Griffiths<sup>1</sup>, P. Eggleton<sup>2</sup>, N. Hemming-Schroeder<sup>3</sup>, T.  
7 Swinfield<sup>4,5</sup>, J. S. Woon<sup>1, 2</sup>, S. D. Allison<sup>3,6</sup>, D.A. Coomes<sup>4</sup>, L. A. Ashton<sup>7</sup> & C.  
8 L. Parr<sup>1,8,9</sup>

10 **Affiliations**

11 <sup>1</sup> School of Environmental Sciences, University of Liverpool, Liverpool, L69 3GP, UK

12 <sup>2</sup> Department of Life Sciences, Natural History Museum, London, UK

13 <sup>3</sup> Department of Earth System Science, University of California, Irvine, CA 92697, USA

14 <sup>4</sup> Department of Plant Sciences, University of Cambridge Conservation Research Institute,  
15 Pembroke Street, Cambridge, CB2 3QZ, UK

16 <sup>5</sup> Centre for Conservation Science, Royal Society for the Protection of Birds, David  
17 Attenborough Building, Pembroke Street, Cambridge, CB2, 3QZ, UK

18 <sup>6</sup> Department of Ecology and Evolutionary Biology, University of California, Irvine, CA  
19 92697, USA

20 <sup>7</sup> School of Biological Sciences, The University of Hong Kong, Hong Kong SAR, China

21 <sup>8</sup> Department of Zoology & Entomology, University of Pretoria, Pretoria, South Africa

22 <sup>9</sup> School of Animal, Plant and Environmental Sciences, University of the Witwatersrand,  
23 Wits, South Africa

24

25 Hannah Griffiths ORCID: 0000-0002-4800-8031

26 **Contact information**

27 Email: [Hannah.griffiths@liverpool.ac.uk](mailto:Hannah.griffiths@liverpool.ac.uk); Tel: +44 151 794 2000

## 28 **Abstract**

29 Tree mortality rates are increasing within tropical rainforests as a result of  
30 global environmental change. When trees die, gaps are created in forest  
31 canopies and carbon is transferred from the living to deadwood pools.  
32 However, little is known about the effect of tree-fall canopy gaps on the  
33 activity of decomposer communities and the rate of deadwood decay in  
34 forests. This means that the accuracy of regional and global carbon  
35 budgets is uncertain, especially given ongoing changes to the structure of  
36 rainforest ecosystems. Therefore, to determine the effect of canopy  
37 openings on wood decay rates and regional carbon flux, we carried out  
38 the first assessment of deadwood mass loss within canopy gaps in old-  
39 growth rainforest. We used replicated canopy gaps paired with closed  
40 canopy sites in combination with macroinvertebrate accessible and  
41 inaccessible woodblocks to experimentally partition the relative  
42 contribution of microbes versus termites to decomposition within  
43 contrasting understory conditions. We show that over a 12-month period,  
44 wood mass loss increased by 63% in canopy gaps compared with closed  
45 canopy sites and that this increase was driven by termites. Using LiDAR  
46 data to quantify the proportion of canopy openings in the study region, we  
47 modelled the effect of observed changes in decomposition within gaps on  
48 regional carbon flux. Overall, we estimate that this accelerated  
49 decomposition increases regional wood decay rate by up to 18.2%,  
50 corresponding to a flux increase of  $0.27 \text{ Mg C ha}^{-1} \text{ yr}^{-1}$  that is not currently  
51 accounted for in regional carbon budgets. These results provide the first  
52 insights into how small-scale disturbances in rainforests can generate

53 hotspots for decomposer activity and carbon fluxes. In doing so, we show  
54 that including canopy gap dynamics and their impacts on wood  
55 decomposition in forest ecosystems could help improve the predictive  
56 accuracy of the carbon cycle in land surface models.

57

58 **Key words**

59 Termites; Invertebrates; Carbon cycling; Carbon modelling; Canopy gap;  
60 Tree mortality; Disturbance; Global change

61

## 62 **Introduction**

63

64 Uncertainty in the behaviour of the carbon cycle is one of the biggest  
65 limiting factors in accurately predicting Earth's temperature into the 21<sup>st</sup>  
66 century (Bodman, Rayner, & Karoly, 2013). Tropical forests hold over half  
67 of global forest carbon stocks ( $471 \pm 93$  PgC), 56% of which is stored in  
68 biomass, and sequester  $1.2 \pm 0.4$  PgC annually (Pan et al., 2011). Recent  
69 work has highlighted how human pressures affect rainforest carbon stocks  
70 in living and dead biomass, showing that selective logging and  
71 degradation increase the proportion of deadwood stocks relative to living  
72 biomass in African and Asian rainforests (Carlson, Koerner, Medjibe,  
73 White, & Poulsen, 2017; Pfeifer et al., 2015).

74

75 Decomposition is the process by which the carbon in dead plant material  
76 is assimilated into soil carbon stores, lost through leaching or released as  
77 CO<sub>2</sub> into the atmosphere through respiration (Cornwell et al., 2009; Swift,  
78 1977). Yet, despite the fact that decomposition has far reaching  
79 implications for global carbon budgets (Hubau et al., 2020), it remains  
80 poorly understood compared with other key ecosystem processes such as  
81 primary production (Harmon, Bond-Lamberty, Tang, & Vargas, 2011).  
82 Furthermore, what is known about the factors controlling deadwood decay  
83 is geographically biased towards temperate regions, with tropical forest  
84 decomposition studies representing just 14% of the published literature  
85 (Harmon et al., 2020). This bias means we lack a basic understanding of

86 the factors that mediate the rate and fate of carbon turnover through  
87 globally important deadwood stocks in tropical rainforests.

88

89 The effect of canopy openness represents an important source of  
90 uncertainty in our understanding of the factors that affect the  
91 decomposition of deadwood in forests (Harmon et al., 2020). This is a  
92 major gap in understanding given that tree mortality rates are rising in  
93 humid tropical forests (McDowell et al., 2018) as a result of increases in  
94 the frequency and severity of hurricanes and drought (Cai et al., 2014);  
95 continued selective logging and degradation (Baccini et al., 2017); and  
96 increases in biotic agents of tree death (liana load, insect outbreaks and  
97 disease; Allen, Breshears & McDowell 2015). Consequently, it is likely that  
98 the size and frequency of rainforest canopy gaps are increasing, along  
99 with concurrent changes in the volume and spatial distribution of  
100 deadwood stocks (Carlson et al., 2017; Pfeifer et al., 2015). However,  
101 because our knowledge of the effect of canopy gaps on deadwood decay  
102 rates is currently limited to just two studies in temperate and boreal  
103 forests (Janisch, Harmon, Chen, Fath, & Sexton, 2005; Shorohova &  
104 Kapitsa, 2014), we lack an empirical evidence base from which to predict  
105 the consequences of ongoing changes to the structure of tropical  
106 rainforests for decomposition and carbon flux. Data shortages such as  
107 these limit the capacity to resolve carbon budget imbalances because  
108 information on how land-surface heterogeneity can affect carbon-cycling  
109 and land-atmosphere interactions is a key area of uncertainty in Earth  
110 system models (Lawrence *et al.* 2019). Therefore, there is a clear need to

111 improve our mechanistic understanding of the drivers of change in  
112 rainforest carbon budgets and thus increase the accuracy and predictive  
113 power of the land surface models included in Earth system models.

114

115 There is mounting evidence that termites along with microbes are the  
116 major agents of deadwood decomposition in rainforest ecosystems (da  
117 Costa, Hu, Li, & Poulsen, 2019; Griffiths, Ashton, Evans, Parr, & Eggleton,  
118 2019; Liu et al., 2015). It is possible that treefall canopy gaps could  
119 negatively or positively affect the activity of both groups. Habitat  
120 disturbance and degradation reduces termite abundance and diversity  
121 (Dibog, Eggleton, Norgrove, Bignell, & Hauser, 1999; Eggleton et al.,  
122 1995; Ewers et al., 2015; Luke, Fayle, Eggleton, Turner, & Davies, 2014;  
123 Tuma et al., 2019) while microbial-mediated nutrient mineralisation rates  
124 decline in response to drought (Yavitt, Wright, & Wieder, 2004). Changes  
125 to the structure of forests caused by removal of trees during selective  
126 logging has been reported to increase microclimate heterogeneity and  
127 create hotter and drier conditions in the forest understory (Blonder et al.,  
128 2018; Hardwick et al., 2015). Therefore, the changes in understory  
129 conditions caused by openings in the canopy when a tree dies could have  
130 major negative effects on both termite and microbial mediated  
131 decomposition. If this is the case, we expect decay rates to slow in canopy  
132 gaps as result of disturbance and unfavourable microclimatic conditions  
133 for the decomposer community. However, an alternative possibility is that  
134 the high concentration of foraging resource (i.e. dead plant matter) in  
135 canopy gaps, that result from tree death, may positively affect

136 decomposition processes by attracting termites and/or stimulating a  
137 positive priming effect within the microbial community (e.g. Lyu et al.,  
138 2018). Under this scenario, we expect to see an increase in decay rates in  
139 canopy gaps in response to elevated resource availability where a tree  
140 has fallen.

141

142 The overarching aim of this investigation was to determine if deadwood  
143 decay rates differ in canopy gaps compared with closed canopy sites in  
144 tropical rainforest. Additionally, we partitioned the relative contribution of  
145 microbes and termites in driving deadwood mass loss in canopy openings  
146 and estimated the effect of any changes in decomposition rates within  
147 canopy gaps on regional carbon flux. To achieve this aim, we used  
148 macroinvertebrate-accessible and inaccessible woodblocks placed within  
149 tree fall canopy gaps and closed canopy sites in an old growth rainforest  
150 in Malaysian Borneo. Furthermore, we assessed the termite community  
151 composition and soil microclimatic conditions within experimental sites  
152 and estimated the volume of deadwood associated with canopy gaps  
153 compared with closed canopy sites. This unique experimental design  
154 allowed us to test alternative hypotheses that deadwood  
155 decomposition in canopy gaps could either: 1) decelerate due to a  
156 negative effect of disturbance and a hotter, drier microclimate (e.g.  
157 Blonder *et al.* 2018) leading to a reduction in the activity of the  
158 decomposer community, or 2) accelerate in response to an influx of dead  
159 plant material attracting termite foraging activity and/or stimulating a  
160 microbial priming effect (e.g. Lyu *et al.* 2018). To scale up our results and



161 place them in a regional context, we used remote sensing (LiDAR) data to  
162 quantify the proportion of canopy openings in the study region and  
163 modelled the effect of observed changes in decomposition within gaps on  
164 regional carbon flux.

165

## 166 **Materials and methods**

### 167 *Study site and gap selection*

168 This study was carried out within an area of lowland, old growth  
169 dipterocarp rainforest in the Maliau Basin Conservation Area, Sabah,  
170 Malaysia (4° 44' 35" to 55" N and 116° 58' 10" to 30" E; mean annual  
171 rainfall 2838 mm  $\pm$  93 mm). On the 20<sup>th</sup> of July 2017, there was a storm at  
172 the study site, which generated winds speeds of 8.4 m/s (Fig. S1). These  
173 were among the strongest winds normally experienced in inland forests of  
174 the region, which placed extreme sheer stress on trees (Jackson et al.,  
175 2020). Consequently, a large number of trees fell within the same 24-hour  
176 period in the study location. Ten tree-fall gaps (mean length: 32 m  $\pm$  2.8,  
177 mean width: 24.5 m  $\pm$  3; see table S1 for gap characteristics) created  
178 during this event were selected for use in this investigation, along with ten  
179 adjacent closed canopy sites, located 20 m from the edge of each gap. We  
180 took 10 hemispherical photos in each gap and closed canopy sites to  
181 quantify canopy openness at each location (see below).

182

### 183 *Decomposition assay*

184 In October 2017, we established a wood decomposition assay. Using a  
185 termite suppression experiment combined with macroinvertebrate

186 accessible and inaccessible mesh bags, Griffiths *et al.* (2019)  
187 demonstrated that non-termite macroinvertebrates did not contribute  
188 significantly to the decomposition of a standardised wood substrate, *Pinus*  
189 *radiata* blocks, at this site. Therefore, to assess the rate of decomposition  
190 within these paired gap and closed canopy sites and determine the  
191 relative contributions of termites versus microbes to the process, we used  
192 the same assay of mass loss from untreated *P. radiata* wood within  
193 macroinvertebrate accessible and inaccessible bags. Wood blocks (9 x 9 x  
194 5 cm,  $161.2 \pm 1.3$  g; wood density of  $0.40 \text{ g cm}^{-3}$  [Zanne *et al.*, 2009]; wood C:N  
195 ratio of  $462 \pm 48$  [Ganjugunte, Condrón, Clinton, Davis, & Mahieu, 2004])  
196 were dried at  $60 \text{ }^{\circ}\text{C}$  until they reached a constant weight and placed  
197 inside “open” (accessible to macroinvertebrates, principally termites, and  
198 microbes), or “closed” (accessible to microbes only) bags, which were all  
199 made with 300 micron nylon mesh (Plastok™, Merseyside, UK). The open  
200 woodblocks had ten 1 cm holes cut into the top and bottom of the bags to  
201 avoid confounding effects of using mesh of different sizes in  
202 decomposition assays (Stoklosa *et al.*, 2016). The edges of the closed  
203 bags were folded several times and sealed with staples to prevent access  
204 by invertebrates. In each gap and closed canopy site, we ran a 50-m  
205 transect and randomly placed 5 open and 5 closed wood blocks 5 m apart  
206 along the transect ( $n = 10$  per site;  $n = 200$  woodblocks in total: 10 x  
207 forest sites x 2 canopy treatments [closed canopy or gap] x 2 mesh  
208 treatments [open or closed] x 5 replicates). Because the gaps were  
209 irregular in shape (Appendix table S1), we placed the transects along the  
210 longest axis of each gap. In all but one of the gap sites, we were unable to

211 establish a 50 m transect, therefore, we placed an additional line  
212 perpendicular to the first, ensuring that each block was always at least 5  
213 m apart from its nearest neighbouring block (Fig. 1).

214

215 A hemispherical photograph was taken by placing an iPhone 6 with a  
216 fisheye lens attachment directly on top of each wood block. Photographs  
217 were analysed using the function *Hemiphot* in R to calculate canopy  
218 openness, which was twice as high within the gaps compared with closed  
219 canopy sites ( $t = 9.67$ ,  $P < 0.001$ , mean openness in gap sites =  $0.24 \pm$   
220  $0.03$ ; mean openness in closed canopy sites =  $0.12 \pm 0.02$ ; Fig. S2). When  
221 placing the woodblocks, the top layer of leaf litter was removed, and the  
222 blocks were put directly on the humus layer. Wood blocks were left on the  
223 forest floor for 12 months (October 2017 to October 2018), after which  
224 they were collected and dried at 60 °C until they reached a constant  
225 weight. Once dried, wood material was separated from termite soil. The  
226 remaining deadwood and termite material (carton and soil) was then re-  
227 weighed separately to calculate the proportion of mass loss from each  
228 block and the mass of soil brought into the mesh bags by termites. Given  
229 that termites are the only invertebrates known to translocate soil into  
230 deadwood (Oberst, Lai, & Evans, 2016), the mass of soil moved into the  
231 experimental woodblocks provides additional information on the termite  
232 activity compared with non-termite wood-feeding invertebrates.

233

234 *Soil conditions and termite communities*

235 Every month for the 12-month duration of the study, soil moisture  
236 percentage and soil temperature were measured within 5 cm of each  
237 wood block using a Delta-T Devices HH2 moisture metre (precise to 0.01  
238 %) and a digital soil thermometer. Measurements were taken in dry  
239 conditions, between 8 AM and 10 AM. To assess termite communities  
240 located within the gap and closed canopy sites, we carried out termite  
241 transects in September 2018 using the Jones and Eggleton transect  
242 method (Jones & Eggleton, 2000). This method uses a 100 m x 2 m belt  
243 transect which is divided into twenty 5 m x 1 m sections. Each section is  
244 sampled for 30 minutes by two trained collectors searching for termites in  
245 twelve 12 cm x 12 cm x 10 cm soil pits and examining all dead wood, leaf  
246 litter and trees for the presence of termites. When encountered, termite  
247 specimens were collected in 70% ethanol and taken to the laboratory for  
248 identification. Because our gap sites were not big enough to place a 100  
249 m transect, we carried out the same method but two using smaller  
250 transects to equal a 50 m transect combined. Therefore the sampling  
251 effort was half that of the Jones & Eggleton (2000) method.

252

### 253 *Quantifying regional gap area*

254 To assess the size and frequency of gaps within Maliau Basin Conservation  
255 Area, we used LiDAR data collected from an airborne survey, which was  
256 carried out by the Natural Environment Research Council (NERC) Airborne  
257 Research Facility (ARF). In November 2014, a Dornier 228-201 was flown  
258 at 1,400-2,400 m a.s.l. with a ground-based Leica base station running  
259 simultaneously to allow sub-meter accuracy and georeferencing of the

260 data. Light detection and ranging data were collected using a Leica  
261 ALS50-II LiDAR sensor, which emits 120 kHz frequency pulses, has a 12°  
262 field of view and a footprint of approximately 40 cm. See Swinfield et al.  
263 (2019) for details of LiDAR data processing to generate canopy height and  
264 digital terrain models at a 0.5 m resolution. Using these data, we analysed  
265 canopy height models to identify gaps, defined as areas with a canopy  
266 height of less than 5 m. Gaps larger than 1 ha were filtered out to remove  
267 LiDAR artefacts, manmade clearances and the river running through  
268 Maliau Basin. We used the package *landscapemetrics* in R and the  
269 thresholds described above to detect gaps and to calculate the area of  
270 each. We then filtered these results to select only gaps that were between  
271 0.025 and 0.16 ha, which is the area range of the gaps forming the basis  
272 of this investigation. This allowed us to assess the total area and  
273 percentage of the landscape likely to be subject to similar microclimatic  
274 conditions to our gap sites at the time of the airborne survey and to  
275 quantify the percentage of gaps that are similar in size to those in this  
276 study.

277

### 278 *Dead wood surveys*

279 To estimate the volume of deadwood found on the forest floor in areas  
280 affected by tree-fall, compared with undisturbed areas, we carried out  
281 deadwood surveys in December 2017. To avoid disturbing our  
282 decomposition assays, these surveys were carried out in areas within the  
283 forest surrounding experimental plots. We established eight 50 m  
284 transects, four of which were within 5 m of a tree that had fallen during

285 the storm in July 2017 and four that were in areas of forest at least 20 m  
286 from the nearest tree fall. Along each transect, we recorded the diameter  
287 of each piece of deadwood that intersected with the line, and these values  
288 were used to calculate the volume of dead wood using the following  
289 equation (Van Wagner 1968):

290

$$291 \quad V = \frac{\pi^2}{8L} \sum d^2$$

292

293 Where  $V$  is the volume of deadwood ( $\text{cm}^3/50 \text{ m}$ ),  $d$  is the diameter of the  
294 deadwood item at the intersection and  $L$  is the length of the sample line.

295

## 296 **Carbon Modelling**

297 A bootstrapping scheme with a million simulations was implemented to  
298 estimate the carbon flux from dead wood and its uncertainty in Maliau  
299 Basin. We estimated carbon fluxes for a completely closed canopy  
300 scenario versus scenarios with observed changes in decay rate and  
301 deadwood volume in canopy openings as well as canopy gap percentages  
302 derived from the remote sensing analysis.

303

### 304 *Wood density*

305 One species, *Pinus radiata*, was used for estimating wood mass loss in our  
306 experiment. Therefore, to account for diversity in wood traits of other  
307 species likely to occur at the study site, we used tree survey data from  
308 Newbery and Lingenfelder (2004) (collected from a lowland dipterocarp

309 forest site within 100 km of our study site). Our bootstrap analysis used  
310 the tree species frequencies from Newbery and Lingenfelder (2004) and  
311 selected a wood density for each species from the Global wood density  
312 database (Zanne et al., 2009). Where wood density for a species was not  
313 available, we randomly selected a wood density value from members of  
314 the same genus within the same region category (South-East Asia  
315 (tropical)). A histogram of the wood density distribution for this study is  
316 shown in Fig. S3. Given that termite and microbial decay rate is negatively  
317 associated with wood density in tropical systems (Liu et al., 2015; Mori et  
318 al., 2014), this approach reduces the possibility that our model  
319 overestimates overall decay rate as a result of the disparity between the  
320 density of our decomposition substrate (*P. radiata*: wood density of 0.40 g  
321 cm<sup>-3</sup>) and the estimated median density of wood from trees in the study  
322 region (0.54 g cm<sup>-3</sup>). We note that the relationship between wood density  
323 and decay rate is less clear in temperate forests (Hu et al., 2018; Kahl et  
324 al., 2017). In addition to wood density, other traits, such as wood  
325 stoichiometry and size of woody substrate (Hu et al., 2018; Kahl et al.,  
326 2017; Oberle et al., 2020), are likely to influence decay rates. However,  
327 information is lacking on how these other traits affect termite-mediate  
328 decay, or wood decomposition more generally in tropical systems.  
329 Therefore, we did not incorporate these factors into our models of regional  
330 carbon fluxes.

331

332 *Scaling decay rates*

333 Liu et al. (2015) is the only study we know of that quantifies how termite-  
334 mediated decay rates depend on wood density. Therefore, we first built a  
335 model to represent wood decay rates under termite attack based on Liu et  
336 al. (2015). We scaled this model to represent wood decay in gaps using  
337 the *P. radiata* wood density and associated decay rate from our study.  
338 Then, we scaled the model again to represent these rates under the  
339 closed canopy. Wood decay rates in forest gaps were based on Liu et al.  
340 (2015) who measured wood traits and decay rates driven by microbes and  
341 termites for 66 species. We fitted an exponential model to decay rates as  
342 a function of wood density using an L1 scheme that minimizes the sum of  
343 the absolute value of the residuals (R package: *L1pack*) (Fig. S4). We used  
344 this scheme, rather than a least-squares approach, to avoid over-  
345 weighting outliers with high decay rates. To obtain a decay rate for each  
346 wood density value, we sampled from a normal distribution with the decay  
347 rate model prediction as the mean and the 68%-confidence interval of the  
348 model fit as the standard deviation (in log space). To avoid biologically  
349 unrealistic decay rates, we truncated the model to the middle 96% of the  
350 modelled decay rate estimates (Fig. S4). Because the model derived from  
351 Liu et al. (2015) predicted a much higher mean decay rate for *P. radiata*  
352 than found in our study (1.3 year<sup>-1</sup> compared with 0.49 year<sup>-1</sup>), we scaled  
353 the model to reflect the *P. radiata* decay rates in the canopy gaps open to  
354 termite activity that we measured in the field. To predict decay rates  
355 under the closed canopy, we also scaled our gap model predictions to  
356 match the decay rates of *P. radiata* open to termite decomposition under  
357 closed canopy in our study. We accounted for random error in this scaling



358 process by sampling our decay rate dataset with  $N(\mu=0.49, \sigma=0.05)$  for  
359 the forest gaps and  $N(\mu=0.30, \sigma=0.04)$  for the closed canopy to obtain a  
360 distribution of scaling factors. These normal distributions were also  
361 truncated to the middle 96% quantile.

362

### 363 *Carbon fluxes*

364 To estimate the deadwood carbon pool at our study site, we used surveys  
365 from Pfeifer *et al.* (2015) from nearby Old Growth plot (OG2) of the  
366 Stability of Altered Forest Ecosystem (SAFE) project, located within Maliau  
367 Basin, <5 km kilometres from our study sites. Pfeifer *et al.* (2015)  
368 estimated there to be  $10.2 \pm 3.5$  Mg C per hectare contained in deadwood  
369 at the OG2. For the bootstrapping scheme, we sampled  $1 \times 10^6$  times from  
370 a normal distribution of wood pools with the corresponding mean and  
371 standard deviation, truncated to the middle 96% quantile. We then  
372 estimated carbon fluxes,  $F$ , for the closed canopy baseline scenario using  
373 the equation

374

$$375 \quad F = k_{canopy} C,$$

376

377 where  $k_{canopy}$  is the decay rate per year under the closed canopy and  $C$  is  
378 the closed canopy carbon pool estimate in megagrams of carbon per  
379 hectare. Because the percentage of canopy gaps is small, we assumed  
380 that the carbon pool estimates from Pfeifer *et al.* (2015) are  
381 representative of the closed canopy. We estimated the carbon flux for our  
382 study site, including canopy gaps, using the following equation:

383

$$384 \quad F^{\dot{c}} = p k_{gaps} \alpha C + (1-p) k_{canopy} C,$$

385

386 where  $F^{\dot{c}}$  is the flux when gaps are included,  $p$  is the proportion of canopy  
387 gaps at the study site,  $k_{gaps}$ , is the decay rate ( $\text{yr}^{-1}$ ) in the canopy gaps and  
388  $\alpha$  is the ratio of the volume of dead wood in the canopy gaps to the  
389 volume of dead wood under the closed canopy. Because the sample size  
390 was small ( $n = 4$ , each) for the volume of dead wood in the canopy gaps  
391 and under the closed canopy, a normal distribution computed from these  
392 data may not be reliable. Therefore, we sampled  $\alpha$  directly from the  
393 dataset for the bootstrapping scheme. Fluxes are reported as geometric  
394 means with geometric standard deviation intervals to best represent the  
395 central tendency of the approximately log-normal bootstrapped  
396 distributions we obtained.

397

### 398 **Statistical analysis**

399 A linear mixed effect model (R package: *LmerTest*) was used to determine  
400 if wood block bag type (macroinvertebrate accessible vs.  
401 macroinvertebrate inaccessible), canopy type (closed canopy vs forest  
402 gap) and the interaction between the two factors affected proportion of  
403 mass lost from wood blocks. Mass loss was logit transformed, which  
404 allowed us to use standard Gaussian linear methods (Warton & Hui, 2011)  
405 and forest site was included as a random factor. To carry out multiple  
406 comparisons of means and identify any differences in wood block mass  
407 loss between bag types and canopy types, we used the *glht* function (R

408 package: *multcomp*) and Tukey contrasts. An Adonis test (package:  
409 *vegan*) was used to assess if the community composition of termites  
410 differed between the closed canopy and forest gap sites, and zero-inflated  
411 generalised linear mixed effects models (R package: *glmmTBM*) were used  
412 to test for differences in the encounter rate of each genus separately in  
413 the closed canopy and forest sites. Linear mixed effects models were used  
414 to test for differences in minimum, mean and maximum soil temperature  
415 and moisture values in closed canopy and gap sites; forest site and  
416 sampling date were included as random factors. Linear mixed models  
417 were used to assess the differences in canopy openness between the  
418 closed canopy and forest gaps, with site included as a random factor.

419

420 Finally, to model the relationship between termite-derived soil recovered  
421 from the woodblocks and woodblock mass loss, while taking into  
422 consideration the high proportion of zeros in the data (50% of open  
423 woodblocks contained no termite-derived soil), we analysed the data in a  
424 two-stage approach following Min & Agresti (2002). First, we created a  
425 binomial variable for the termite soil mass, where woodblocks containing  
426 no soil received a 0 and those with more than zero grams of soil received  
427 a 1. We then fit the data to a generalised linear mixed effect model  
428 (glmer) with site included as a random factor, to test if the proportion of  
429 wood mass lost (logit transformed) had a significant effect on the  
430 probability of a woodblock containing termite soil. Next, we removed the  
431 zero soil values from the dataset and ran a linear mixed effects model  
432 (lmer) on only woodblocks from which we recovered soil, to assess if logit

433 transformed wood mass loss was significantly associated with the mass of  
434 soil that was recovered from the woodblocks. Again, site was included as  
435 a random factor. This approach overcame the problem of modelling zero-  
436 inflated data (only invertebrate accessible bags were included in these  
437 models because no soil was recovered from closed bags).

438

## 439 **Results**

### 440 *Decomposition*

441 Significantly more mass was lost from open woodblocks (accessible to  
442 both microbes and macroinvertebrates) in forest gaps (mean mass loss  
443 over 12 months:  $49\% \pm 5\%$ ) compared with open woodblocks in closed  
444 canopy sites (mean mass loss:  $30\% \pm 4\%$ ;  $z = 3.8$ ,  $P < 0.001$ ). This is an  
445 increase in decomposition by a factor of 1.63 in forest where both  
446 microbes and macroinvertebrates have access to the woodblocks (Fig. 2).  
447 In both the closed canopy and gaps sites, the presence of  
448 macroinvertebrates significantly increased the proportion of mass lost, but  
449 the magnitude of this increase was greater in forest gaps, as indicated by  
450 significant interaction between woodblock bag type and canopy type (LRT  
451  $= 4.18$ ,  $P = 0.04$ ): woodblock mass loss increased by a factor of 2 in open  
452 (mean mass loss:  $30 \pm 4\%$ ) compared with closed bags (mean mass loss:  
453  $15 \pm 2\%$ ) in closed canopy sites ( $z = 3.08$ ,  $P = 0.01$ ), but increased by a  
454 factor of 2.58 within open (mean mass loss:  $49 \pm 5\%$ ) versus closed bags  
455 ( $19 \pm 2\%$ ) in forest gaps ( $z = 5.9$ ,  $P < 0.001$ ). We found a significant  
456 positive relationship between woodblock mass loss and the likelihood that  
457 a wood block contained termite-derived soil and carton within the open

458 bags ( $z = 4.19$ ,  $P < 0.001$ ; Fig S5), and a significant positive relationship  
459 between the proportion of mass lost from a woodblock and the mass of  
460 dry soil recovered from bags containing soil ( $z = 2.94$ ,  $P = 0.005$ ; Fig. S5);  
461 indicating that termites, rather than other macro-invertebrates, were  
462 responsible for this mass loss. There was no significant difference in mass  
463 lost from closed woodblocks in the closed canopy compared with closed  
464 woodblocks in forest gap sites ( $z = 0.86$ ,  $P = 0.83$ ), suggesting that  
465 changes in microbial activity were not responsible for the increase  
466 decomposition in the gaps (Fig. 2).

467

#### 468 *Soil microclimate and termite communities*

469 We found small but significant differences in soil temperature and soil  
470 moisture within closed canopy and forest gap sites. The soil in gaps  
471 tended to be warmer and wetter. Minimum soil temperature was higher by  
472  $0.5^{\circ}\text{C}$  and mean soil temperature was  $0.3^{\circ}\text{C}$  higher in gaps compared with  
473 closed canopy sites. There was no significant difference in maximum soil  
474 temperature. Minimum, mean and maximum soil moisture were higher in  
475 canopy gaps compared with non-gap sites by 2, 1.5 and 3.5 percentage  
476 points, respectively (Fig. 3; Table 1). We found no difference in the  
477 composition of termite communities collected in the closed canopy  
478 compared with forest gaps sites nor was there any difference in the  
479 number of encounters of individual genera in the two canopy types (Fig.  
480 S6).

481

#### 482 *Gap area and carbon modelling*

483 Within the LiDAR surveyed area of 940 ha of lowland tropical rainforest,  
484 we detected a total of 20,928 gaps, with the centre of the cumulative  
485 distribution of gaps (i.e. the point where half of the gap area is comprised  
486 of smaller gaps and the remaining half by larger gaps) at 122 m<sup>2</sup> (0.01 ha)  
487 and covering a cumulative area of 24 ha, or 2.5% of the study site. Of  
488 these, 128 gaps were of comparable size to those used in this study  
489 (between 0.025 and 0.16 ha). These gaps covered a cumulative area of  
490 6.5 ha, which is 0.7 % of the surveyed area and represents 27% of the  
491 total gap area in the study region (Fig. 4). In the forest matrix immediately  
492 surrounding our experimental plots, we found 187% more deadwood in  
493 areas affected by tree fall compared with undisturbed areas (average  
494 volume in areas more than 20 m from tree fall:  $95.4 \pm 36.6$  cm<sup>3</sup> per 50 m  
495 transect; average volume in areas close to tree fall:  $272.9 \pm 98.7$  cm<sup>3</sup> per  
496 50 m transect; Fig. 5).

497

498 Our initial model applied the changes in decay rate and wood pools to  
499 canopy gaps covering 0.7% of the surveyed area, which is the cumulative  
500 area that includes gaps of the same size as those forming the basis of this  
501 investigation: 128 gaps in total, measuring between 0.025 and 0.16 ha.  
502 Under this assumption of gap area, deadwood carbon fluxes increased  
503 above baseline by a geometric mean value of 5.7% with a geometric SD  
504 interval of -3.1% to 15.2%, corresponding to a flux increase of 0.09 Mg C  
505 ha<sup>-1</sup> yr<sup>-1</sup> (Table 2). If we assumed changes in wood pools and decay rates  
506 applied to all gaps detected by LiDAR, i.e. 2.5% of the survey area, then  
507 the flux increase was 18.2% (geometric SD interval of -15.4% to 47.7%),

508 or 0.27 Mg C ha<sup>-1</sup> yr<sup>-1</sup>. Increases in both wood pool sizes and termite-  
509 driven decay rates in gaps contributed to the higher fluxes relative to the  
510 baseline scenario with no gaps (Fig. S10). At the scale of the 940 ha  
511 region of our LiDAR analysis, gap-driven fluxes increased from 1380 Mg C  
512 ha<sup>-1</sup> yr<sup>-1</sup> to 1460 Mg C yr<sup>-1</sup> for the 0.7% gap scenario and to 1640 Mg C ha<sup>-1</sup>  
513 yr<sup>-1</sup> for the 2.5% gap scenario.

514

## 515 **Discussion**

516 We found that deadwood decomposition in a lowland tropical rainforest  
517 increased by approximately two thirds in tree-fall canopy gaps, compared  
518 with closed-canopy forest, and that this accelerated decomposition was  
519 driven by termites. These results add to a growing body of evidence  
520 showing that termites are major drivers of deadwood decomposition in  
521 tropical rainforests (Griffiths et al., 2019; Law et al., 2019) and that their  
522 importance for the maintenance of ecological processes can increase in  
523 response to environmental perturbations (Ashton et al., 2019). The  
524 functioning of canopy gaps as hotspots for carbon cycling has important  
525 implications for land-surface model development given that tree mortality  
526 is increasing in rainforests (Brienen et al., 2015; Hubau et al., 2020;  
527 McDowell et al., 2018), which will increase the number of gaps, and  
528 cumulative area of forest affected by canopy openings.

529

530

531

532 *Drivers of increased decomposition*

533 We hypothesized that changes in deadwood stocks and microclimate in  
534 gaps might alter wood decomposition fluxes. Deadwood stocks were three  
535 times higher in canopy gaps than in closed canopy sites. Microbial  
536 decomposition did not differ between contrasting canopy conditions while  
537 termite-mediated decay increased by almost two thirds in tree-fall gaps.  
538 The small but significant differences we detected in the soil microclimate  
539 of our gap and closed canopy sites had no effect on microbial decay but  
540 may have led to an increase in termite-mediated decay. Combined, these  
541 results point to an influx of deadwood foraging material for termites as a  
542 likely driver of the increased decomposition in gaps we detected.  
543 However, because this hypothesis needs further testing, this work serves  
544 as a platform from which the mechanisms behind the patterns we report  
545 can be rigorously tested and a starting point for incorporation of these  
546 patterns into global carbon models.

547

548 We found no support for our hypothesis that shifts in microclimate and/or  
549 disturbance caused by tree mortality are detrimental to the decomposer  
550 community. Neither termite nor microbial-mediated wood mass loss  
551 declined beneath canopy gaps. Soil conditions in our focal canopy gaps  
552 were not as we predicted: although slightly warmer, they were wetter,  
553 rather than drier than in the paired closed canopy sites. This result could,  
554 in part, explain the lack of disturbance/microclimate effect detected on  
555 the decomposer community because we have no *a priori* reason to believe  
556 that these small increases in soil moisture would negatively affect  
557 microbial or termite activity.



558

559 Our finding of increased termite-mediated decay in canopy gaps supports  
560 our alternative hypothesis that an increase in termite food sources  
561 (deadwood) in tree fall gaps attracts more termites to these areas, which  
562 leads to increased decomposition. We found almost three times more  
563 deadwood on the forest floor in areas close to tree fall (Fig. 5), and we  
564 propose that this influx of wood is likely to have led to an increase in  
565 termite foraging in the gap sites. This finding has important implications  
566 for the way in which decomposition models are parameterised in  
567 rainforest systems because our results suggest that carbon flux rates from  
568 deadwood are not only a function of the proportion of wood necromass in  
569 the system (Rice et al., 2004) but may also be mediated by the spatial  
570 clustering of the deadwood resource. Given that microbial decay rates did  
571 not change in the canopy gaps, we found no evidence to suggest the  
572 clustering/influx of dead plant resources had a comparable positive effect  
573 on the microbial decomposer community.

574

575 We are confident that termites were responsible for the invertebrate  
576 driven increase in decomposition because a previous study, which used  
577 macroinvertebrate accessible and inaccessible woodblock bags, in  
578 combination with a large-scale suppression of termite communities,  
579 demonstrated that non-termite macroinvertebrates do not contribute  
580 significantly to wood decay at this site Griffiths et al., (2019). Our present  
581 study exactly mimics the experimental design used to manipulate the  
582 macroinvertebrate community access to wood blocks in the previous

583 work. Therefore, we conclude that termites were responsible for the  
584 elevated mass loss from wood within the macroinvertebrate accessible  
585 bags. Moreover, we found a significant positive relationship between the  
586 probability that a wood block contained termite-derived soil and  
587 proportion wood mass loss, as well as a positive relationship between the  
588 mass of soil brought into our open woodblock bags and wood block mass  
589 loss (no soil was recovered from closed woodblocks; Fig. S5). This  
590 relationship provides further evidence that termites are the main drivers  
591 of the observed wood mass loss from the macroinvertebrate accessible  
592 bags because termites are the only decomposer organism known to  
593 move clay and soil around in this way (Oberst et al., 2016). Because our  
594 sampling to assess the composition and biomass of termites within the  
595 gap and closed canopy sites was carried out 15-months after the storm  
596 that created the focal gaps and influx of deadwood material, it seems  
597 likely that we missed the increase in termite activity within the gap sites  
598 that we hypothesise led to the elevated decay rate within our gaps.  
599 Further work is needed to conclusively disentangle the possible drivers of  
600 the increased termite activity and wood decay rates in canopy gaps  
601 (microclimate versus increased food supply). Our findings highlight the  
602 need to explicitly test the influence of microclimate versus deadwood  
603 volume on decay rates in field experiments. This would allow us to gain a  
604 deeper understanding of the factors mediating decomposition and carbon  
605 balance in rainforest ecosystems.

606

607 *Implications for rainforest carbon flux and sources of uncertainties*

608 We show that termite-mediated deadwood decay responds positively to  
609 small-scale disturbances within old-growth rainforest. This suggests that  
610 accelerated termite decomposition could be a key driver of observed  
611 elevated carbon fluxes caused by increased tree mortality and  
612 degradation within standing tropical forests (Baccini et al., 2017; Hubau et  
613 al., 2020). As such, these results add to our understanding of the biotic  
614 mechanisms underpinning ongoing changes to rainforest carbon budgets.  
615 However, the resilience of termite-mediated ecosystem processes to  
616 differing disturbance thresholds is largely unknown (but see Tuma *et al.*  
617 2019). Recent work has shown that termites maintain leaf litter  
618 decomposition, nutrient heterogeneity and soil moisture retention in old  
619 growth forest during periods of drought (Ashton et al., 2019), indicating  
620 that they can provide ecosystem resilience to climate change.  
621 Understanding the extent to which the resilience provided by termites is  
622 maintained in degraded habitats is key to the on-going improvement of  
623 land-surface models as well the development of land-management  
624 practices aimed at increasing the resilience of tropical landscapes under  
625 ongoing environmental change

626

627 Given the vast amounts of carbon contained within tropical forests (Lewis,  
628 Edwards, & Galbraith, 2015; Pan et al., 2011), even a relatively small  
629 change in C flux due to termite-mediated decomposition in canopy gaps  
630 may scale up to large differences over tropical biomes. For example, our  
631 estimated flux increase of  $0.27 \text{ Mg C ha}^{-1} \text{ yr}^{-1}$  represents 2% of total net  
632 primary productivity ( $13.5 \text{ Mg C ha}^{-1} \text{ yr}^{-1}$ ) measured in lowland rainforests

633 of Malaysian Borneo (Riutta et al., 2018). This timely finding is of  
634 particular relevance given that the Community Land Model version 6  
635 (CLM6) is currently under development, which will include additional  
636 parameterisation of ecosystem processes that influence the cycling of C  
637 through terrestrial ecosystems and build upon progress made in CLM5  
638 (Lawrence et al., 2019). However, although our analysis indicated the  
639 potential for substantial increases in carbon flux due to changes in termite  
640 activity in canopy gaps, the variance around the estimated magnitude of  
641 this change in flux remains high due to a number of potential sources of  
642 uncertainty in our model.

643

644 Lack of data on how climate mediates the relationship between termite-  
645 driven decay and wood density represents an area of uncertainty in our  
646 model estimates and contributes to the large confidence intervals  
647 associated with our C-flux estimates. Our estimate of termite-mediated  
648 decay associated with the varying wood densities is reliant on an  
649 empirical model we fitted to a single dataset of decay rates from a distant  
650 study site in Yunnan Province, China (Liu et al., 2015). While both are  
651 Asian tropical rainforests, the climate differs between the two regions:  
652 mean annual rainfall of 1463 mm versus 2838 mm and average monthly  
653 temperatures of 21.7°C versus 24.9°C in Yunan (Li et al., 2012) and Maliau  
654 (Law et al., 2019), respectively. These climatic differences could be  
655 important because while some studies suggest that wood traits are key  
656 drivers of deadwood decay (Hu et al., 2018; Zanne et al., 2015), others  
657 have found stronger relationships with climate (Chambers, Higuchi,

658 Schimel, Ferreira, & Melack, 2000; Pietsch et al., 2019). Consequently, it is  
659 possible that the effect of wood density on rate of termite mediated decay  
660 could differ between the two regions.

661

662 Wood density is not the only trait known to influence decay rates. Results  
663 from studies focussed on microbial wood decomposition in temperate  
664 regions show that a range of other traits can also significantly effect wood  
665 decay, either positively (e.g. phosphorous, nitrogen) or negatively (e.g.  
666 bark ratio, lignin concentration [Kahl et al., 2017; Oberle et al., 2019]).  
667 Furthermore, a recent meta-analysis (Hu et al., 2018), highlighted the  
668 importance of wood size (diameter) and nitrogen concentration in  
669 controlling wood decay globally. We acknowledge that termite-mediated  
670 decay rates could also be influenced by these wood traits and our models  
671 may be improved if more data were available on the effect of wood  
672 stoichiometry on termite attack rate in our system. However, data on  
673 wood chemical traits within our study region are currently unavailable, but  
674 Martin, Erickson, Kress, & Thomas (2014) provide an overview of wood  
675 nitrogen concentration and correlations between nitrogen and other wood  
676 traits for 59 Panamanian tree species. This work reveals a mean wood C:N  
677 ratio for these neo-tropical tree species of  $278 \pm 32$ , with values ranging  
678 from 84.7 to 1360.8, and a positive relationship between wood density  
679 and wood nitrogen concentration. Our wood decomposition substrate  
680 (*Pinus radiata*) falls within this range with a C:N of 462 (Ganjegunte et al.,  
681 2004).

682

683 We are aware of no study that has interrogated the influence of wood  
684 chemical traits on termite mediated decomposition; therefore, we are  
685 unable to speculate as to how these factors could influence our flux  
686 estimate. However, Ulyshen, Müller, & Seibold (2016) show that termite-  
687 mediated wood mass loss increased significantly where bark was present,  
688 which is in contrast to the findings presented by Kahl et al., (2017) who  
689 show that higher bark ratio negatively affected microbial decay rates. It is  
690 important to note that our use of wood blocks of a uniform (small) size  
691 and lacking in bark could have resulted in elevated mass loss compared to  
692 larger woody substrates with intact bark. However, our wood substrate  
693 was chosen to allow for standardization and to facilitate comparison  
694 across our experimental sites and treatments. Therefore, we highlight the  
695 need for additional work to partition the contributions of microbes versus  
696 termites in the decomposition of deadwood with a range of traits and in a  
697 range of ecosystems to facilitate the development of more precise models  
698 of wood decomposition and carbon cycling.

699

700 Possible inaccuracies in our estimates of deadwood on the forest floor are  
701 another potential source of error in our model estimates. We reported that  
702 the volume of deadwood was 187% higher in areas affected by treefall  
703 compared with those unaffected, using field transects 5-months after the  
704 storm that created the canopy gaps. However, it is possible that termite-  
705 mediated wood removal in that 5-month period, in response to the influx  
706 of foraging material, removed deadwood disproportionately from the tree-  
707 fall sites. This would result in an underestimation of the difference in wood

708 volume in contrasting canopy environments, with potentially more  
709 deadwood in recently created gaps than we reported. Further, we used  
710 data from Pfeifer *et al.* (2015) to describe the deadwood carbon pool  
711 under closed canopy conditions. However, Pfeifer *et al.* (2015) reported  
712 different deadwood carbon estimates from two sites, both within 3.2 km of  
713 our study site (“OG1”: 27.05 Mg C per ha, and “OG2”: 10.24 Mg per ha).  
714 We used values from the site closest to our experimental plots (< 1km),  
715 OG 2, which was the lowest carbon pool value and thus avoids inflated  
716 estimates of the effect of termites on regional C flux. However, the higher  
717 deadwood carbon pool reported from Old Growth 1 combined with the  
718 possibility that we underestimated the proportional difference in  
719 deadwood volume in gaps versus closed canopy sites suggests that our  
720 modelling effort is a conservative estimate of the true effect of termite  
721 mediated C flux in canopy gaps.

722

723 Finally, difficulties in describing temporally and spatially representative  
724 forest canopy gap fractions may have contributed model inaccuracies.  
725 Using data from the aerial survey carried out in November 2014, we found  
726 the cumulative area of canopy gaps in the study region to be between 0.7  
727 and 2.5%. This range is within the lower bounds of canopy gap fractions  
728 described by Hunter *et al.* (2015) in the Amazon rainforest (2-5%) and  
729 smaller than that reported by Yavitt *et al.* (1995) within a Panamanian  
730 forest (4%). Small canopy openings in rainforest ecosystems caused by  
731 isolated tree fall events rapidly become colonised by lateral canopy  
732 growth, meaning that their detectability using remote sensing quickly

733 decreases with time since gap creation (Asner, Keller, & Silva, 2004). The  
734 aerial survey used in this investigation was not, as far as we are aware,  
735 carried out soon after an intense storm similar to the storm that created  
736 the focal gaps in this study. Therefore, our gap fraction estimate is likely  
737 to be smaller than if it been carried out immediately following the storm  
738 that formed the basis of this investigation. However, despite these  
739 uncertainties, our analysis demonstrates that canopy gaps in rainforest  
740 ecosystems function as hotspots of deadwood decay, which has far  
741 reaching implications for regional and global budgeting.

742

#### 743 *Conclusion*

744 To our knowledge, this is the first study to show that rainforest treefall  
745 canopy gaps represent hotspots for deadwood decay and carbon cycling.  
746 We provide insights into the relative importance of invertebrates  
747 compared with microbes in driving the decomposition of deadwood,  
748 adding to a growing body of literature showing that termites and their  
749 mutualistic microbes are equally, if not more important than free-living  
750 microorganisms for deadwood decay in rainforests (Griffiths et al., 2019;  
751 Law et al., 2019). These results demonstrate that to improve the accuracy  
752 of carbon modelling, a variable rate of decomposition should be included  
753 in model parameters to account for accelerated termite-mediated decay  
754 within tree fall canopy gaps. However, we urgently require information on  
755 the effect of a variety of wood traits on termite-mediated decay rates, as  
756 well as research efforts to quantify whether these patterns of accelerated  
757 decomposition hold true in selectively logged forest or oil palm



758 plantations. Only through addressing these knowledge gaps will we be  
759 able to reduce model uncertainties and accurately predict how ongoing  
760 changes to tropical landscapes will affect global carbon cycling, climate  
761 and the functioning and maintenance of vitally important tropical  
762 rainforest ecosystems.

763

## 764 **Acknowledgements**

765 We are extremely grateful to our field assistants R. Binti Manber, Lawlina  
766 Mansul and Donny Banasib for their tireless hard work in the field, which  
767 made this study possible. We thank G. Reynolds, U. Jami and A. Karolus  
768 for coordinating fieldwork. This work was supported by the South East  
769 Asian Rainforest Research Partnership (SEARRP), with permission from  
770 Maliau Basin Management Committee and the Sabah Biodiversity Council.  
771 We thank the funding bodies that financially supported this work: The  
772 Leverhulme Trust, research grant: RPG-2017-271 awarded to KP; National  
773 Science Foundation, Research Traineeship 1633631 to NHS, and National  
774 Science Foundation, grant DEB-1655340 to SDA.

775

## 776 **Data Sharing and Accessibility**

777 The data that support the findings of this study are openly available in  
778 Dryad data repository at [http://doi.org/\[doi\]](http://doi.org/[doi]), reference number [reference  
779 number].

780

## 781 **References**

782 Allen, C. D., Breshears, D. D., & McDowell, N. G. (2015). On

783 underestimation of global vulnerability to tree mortality and forest die-  
784 off from hotter drought in the Anthropocene. *Ecosphere*, 6(8), 1–55.  
785 <https://doi.org/10.1890/ES15-00203.1>

786 Ashton, L. A., Griffiths, H. M., Parr, C. L., Evans, T. A., Didham, R. K.,  
787 Hasan, F., ... Eggleton, P. (2019). Termites mitigate the effects of  
788 drought in tropical rainforest. *Science*, 177(January), 174–177.

789 Asner, G. P., Keller, M., & Silva, J. N. M. (2004). Spatial and temporal  
790 dynamics of forest canopy gaps following selective logging in the  
791 eastern Amazon. *Global Change Biology*, 10(5), 765–783.  
792 <https://doi.org/10.1111/j.1529-8817.2003.00756.x>

793 Baccini, A., Walker, W., Carvalho, L., Farina, M., Sulla-Menashe, D., &  
794 Houghton, R. A. (2017). Tropical forests are a net carbon source based  
795 on aboveground measurements of gain and loss. *Science*,  
796 358(October), 230–234.

797 Blonder, B., Both, S., Coomes, D. A., Elias, D., Jucker, T., Kvasnica, J., ...  
798 Svátek, M. (2018). Extreme and Highly Heterogeneous Microclimates  
799 in Selectively Logged Tropical Forests. *Frontiers in Forests and Global*  
800 *Change*, 1(October), 1–14. <https://doi.org/10.3389/ffgc.2018.00005>

801 Bodman, R. W., Rayner, P. J., & Karoly, D. J. (2013). Uncertainty in  
802 temperature projections reduced using carbon cycle and climate  
803 observations. *Nature Climate Change*, 3(8), 725–729.  
804 <https://doi.org/10.1038/nclimate1903>

805 Brienen, R. J. W., Phillips, O. L., Feldpausch, T. R., Gloor, E., Baker, T. R.,  
806 Lloyd, J., ... Zagt, R. J. (2015). Long-term decline of the Amazon carbon  
807 sink. *Nature*, 519(7543), 344–348.

808 <https://doi.org/10.1038/nature14283>

809 Cai, W., Borlace, S., Lengaigne, M., Van Rensch, P., Collins, M., Vecchi, G.,  
810 ... Jin, F. F. (2014). Increasing frequency of extreme El Niño events due  
811 to greenhouse warming. *Nature Climate Change*, 4(2), 111–116.  
812 <https://doi.org/10.1038/nclimate2100>

813 Carlson, B. S., Koerner, S. E., Medjibe, V. P., White, L. J. T., & Poulsen, J. R.  
814 (2017). Deadwood stocks increase with selective logging and large  
815 tree frequency in Gabon. *Global Change Biology*, 23(4), 1648–1660.  
816 <https://doi.org/10.1111/gcb.13453>

817 Chambers, J. Q., Higuchi, N., Schimel, J. P., Ferreira, L. V, & Melack, J. M.  
818 (2000). Decomposition and carbon cycling of dead trees in tropical  
819 forests of the central Amazon. *Oecologia*, 122(3), 380–388.  
820 <https://doi.org/10.1007/s004420050044>

821 Cornwell, W. K., Cornelissen, J. H. C., Allison, S. D., Bauhus, J., Eggleton, P.,  
822 Preston, C. M., ... Zanne, A. E. (2009). Plant traits and wood fates  
823 across the globe: Rotted, burned, or consumed? *Global Change*  
824 *Biology*, 15(10), 2431–2449. [https://doi.org/10.1111/j.1365-](https://doi.org/10.1111/j.1365-2486.2009.01916.x)  
825 [2486.2009.01916.x](https://doi.org/10.1111/j.1365-2486.2009.01916.x)

826 da Costa, R. R., Hu, H., Li, H., & Poulsen, M. (2019). Symbiotic plant  
827 biomass decomposition in Fungus-Growing termites. *Insects*, 10(4), 1–  
828 15. <https://doi.org/10.3390/insects10040087>

829 Dibog, L., Eggleton, P., Norgrove, L., Bignell, D. E., & Hauser, S. (1999).  
830 Impacts of canopy cover on soil termite assemblages in an  
831 agrisilvicultural system in southern Cameroon. *Bulletin of*  
832 *Entomological Research*, 89(02), 125–132.

833 <https://doi.org/10.1017/S0007485399000206>

834 Eggleton, P., Bignell, D. E., Sands, W. A., Waite, B., Wood, T. G., & Lawton,  
835 J. H. (1995). The species richness of termites (isoptera) under differing  
836 levels of forest disturbance in the mbalmayo forest reserve, southern  
837 cameroon. *Journal of Tropical Ecology*, 11(1), 85–98.  
838 <https://doi.org/10.1017/S0266467400008439>

839 Ewers, R. M., Boyle, M. J. W., Gleave, R. A., Plowman, N. S., Benedick, S.,  
840 Bernard, H., ... Turner, E. C. (2015). Logging cuts the functional  
841 importance of invertebrates in tropical rainforest. *Nature*  
842 *Communications*, 6, 6836. <https://doi.org/10.1038/ncomms7836>

843 Ganjegunte, G. K., Condrón, L. M., Clinton, P. W., Davis, M. R., & Mahieu,  
844 N. (2004). Decomposition and nutrient release from radiata pine  
845 (*Pinus radiata*) coarse woody debris. *Forest Ecology and Management*,  
846 187(2–3), 197–211. [https://doi.org/10.1016/S0378-1127\(03\)00332-3](https://doi.org/10.1016/S0378-1127(03)00332-3)

847 Griffiths, H. M., Ashton, L. A., Evans, T. A., Parr, C. L., & Eggleton, P.  
848 (2019). Termites can decompose more than half of deadwood in  
849 tropical rainforest. *Current Biology*, 29, 118–119.  
850 <https://doi.org/10.1016/j.cub.2019.01.012>

851 Hardwick, S. R., Toumi, R., Pfeifer, M., Turner, E. C., Nilus, R., & Ewers, R.  
852 M. (2015). The relationship between leaf area index and microclimate  
853 in tropical forest and oil palm plantation: Forest disturbance drives  
854 changes in microclimate. *Agricultural and Forest Meteorology*, 201,  
855 187–195. <https://doi.org/10.1016/j.agrformet.2014.11.010>

856 Harmon, M. E., Bond-Lamberty, B., Tang, J., & Vargas, R. (2011).  
857 Heterotrophic respiration in disturbed forests: A review with examples

858 from North America. *Journal of Geophysical Research: Biogeosciences*,  
859 116(2), 1-17. <https://doi.org/10.1029/2010JG001495>

860 Harmon, M. E., Fasth, B. G., Yatskov, M., Kastendick, D., Rock, J., &  
861 Woodall, C. W. (2020). Release of coarse woody detritus - related  
862 carbon : a synthesis across forest biomes. *Carbon Balance and*  
863 *Management*, 1-21. <https://doi.org/10.1186/s13021-019-0136-6>

864 Hu, Z., Michaletz, S. T., Johnson, D. J., McDowell, N. G., Huang, Z., Zhou,  
865 X., & Xu, C. (2018). Traits drive global wood decomposition rates more  
866 than climate. *Global Change Biology*, 24(11), 5259-5269.  
867 <https://doi.org/10.1111/gcb.14357>

868 Hubau, W., Lewis, S. L., Phillips, O. L., Affum-Baffoe, K., Beeckman, H.,  
869 Cuní-Sanchez, A., ... Zemagho, L. (2020). Asynchronous carbon sink  
870 saturation in African and Amazonian tropical forests. *Nature*,  
871 579(7797), 80-87. <https://doi.org/10.1038/s41586-020-2035-0>

872 Hunter, M. O., Keller, M., Morton, D., Cook, B., Lefsky, M., Ducey, M., ...  
873 Zang, R. (2015). Structural dynamics of tropical moist forest gaps.  
874 *PLoS ONE*, 10(7), 1-19. <https://doi.org/10.1371/journal.pone.0132144>

875 Jackson, T. ., Shenkin, A. ., Majalap, N., Jami, J. ., Sailim, A. B., Reynolds,  
876 G., ... Disney, M. (2020). The mechanical stability of the world's tallest  
877 broadleaf trees. *The Mechanical Stability of the World's Tallest*  
878 *Broadleaf Trees*, 00, 1-11. <https://doi.org/10.1101/664292>

879 Janisch, J. E., Harmon, M. E., Chen, H., Fasth, B., & Sexton, J. (2005).  
880 Decomposition of coarse woody debris originating by clearcutting of  
881 an old-growth conifer forest. *Écoscience*, 12(2), 151-160.  
882 <https://doi.org/10.2980/i1195-6860-12-2-151.1>

883 Jones, D. T., & Eggleton, P. (2000). Sampling termite assemblages in  
884 tropical forests: Testing a rapid biodiversity assessment protocol.  
885 *Journal of Applied Ecology*, 37(1), 191–203.  
886 <https://doi.org/10.1046/j.1365-2664.2000.00464.x>

887 Kahl, T., Arnstadt, T., Baber, K., Bässler, C., Bauhus, J., Borken, W., ...  
888 Gossner, M. M. (2017). Wood decay rates of 13 temperate tree species  
889 in relation to wood properties, enzyme activities and organismic  
890 diversities. *Forest Ecology and Management*, 391, 86–95.  
891 <https://doi.org/10.1016/j.foreco.2017.02.012>

892 Law, S., Eggleton, P., Griffiths, H., Ashton, L., & Parr, C. (2019). Suspended  
893 Dead Wood Decomposes Slowly in the Tropics , with Microbial Decay  
894 Greater than Termite Decay. *Ecosystems*, (June).  
895 <https://doi.org/10.1007/s10021-018-0331-4>

896 Lawrence, D. M., Fisher, R. A., Koven, C. D., Oleson, K. W., Swenson, S. C.,  
897 Bonan, G., ... Zeng, X. (2019). The Community Land Model Version 5:  
898 Description of New Features, Benchmarking, and Impact of Forcing  
899 Uncertainty. *Journal of Advances in Modeling Earth Systems*, 11(12),  
900 4245–4287. <https://doi.org/10.1029/2018MS001583>

901 Lewis, S. L., Edwards, D. P., & Galbraith, D. (2015). Increasing human  
902 dominance of tropical forests. *Science*, 349, 827–832.

903 Li, R., Luo, G., Meyers, P. A., Gu, Y., Wang, H., & Xie, S. (2012). Leaf wax n-  
904 alkane chemotaxonomy of bamboo from a tropical rain forest in  
905 Southwest China. *Plant Systematics and Evolution*, 298(4), 731–738.  
906 <https://doi.org/10.1007/s00606-011-0584-2>

907 Liu, G., Cornwell, W. K., Cao, K., Hu, Y., Van, R. S. P., Yang, S., ...

908 Cornelissen, J. H. C. (2015). Termites amplify the effects of wood traits  
909 on decomposition rates among multiple bamboo and dicot woody  
910 species. *Journal of Ecology*, *103*, 1214–1223.  
911 <https://doi.org/10.1111/1365-2745.12427>

912 Luke, S. H., Fayle, T. M., Eggleton, P., Turner, E. C., & Davies, R. G. (2014).  
913 Functional structure of ant and termite assemblages in old growth  
914 forest, logged forest and oil palm plantation in Malaysian Borneo.  
915 *Biodiversity and Conservation*, *23*(11), 2817–2832.  
916 <https://doi.org/10.1007/s10531-014-0750-2>

917 Lyu, M., Xie, J., Vadeboncoeur, M. A., Wang, M., Qiu, X., Ren, Y., ...  
918 Kuzyakov, Y. (2018). Simulated leaf litter addition causes opposite  
919 priming effects on natural forest and plantation soils. *Biology and*  
920 *Fertility of Soils*, *54*(8), 925–934. [https://doi.org/10.1007/s00374-018-](https://doi.org/10.1007/s00374-018-1314-5)  
921 [1314-5](https://doi.org/10.1007/s00374-018-1314-5)

922 Martin, A. R., Erickson, D. L., Kress, W. J., & Thomas, S. C. (2014). Wood  
923 nitrogen concentrations in tropical trees: phylogenetic patterns and  
924 ecological correlates. *New Phytologist*, *205*, 484–495.

925 McDowell, N., Allen, C. D., Anderson-Teixeira, K., Brando, P., Brienen, R.,  
926 Chambers, J., ... Xu, X. (2018). Drivers and mechanisms of tree  
927 mortality in moist tropical forests. *New Phytologist*, *219*(3), 851–869.  
928 <https://doi.org/10.1111/nph.15027>

929 Min, Y., & Agresti, A. (2002). Modeling Nonnegative Data with Clumping at  
930 Zero : A Survey Models for Semicontinuous Data. *Jirss*, *1*(May), 7–33.

931 Mori, S., Itoh, A., Nanami, S., Tan, S., Chong, L., & Yamakura, T. (2014).  
932 Effect of wood density and water permeability on wood decomposition

933 rates of 32 bornean rainforest trees. *Journal of Plant Ecology*, 7(4),  
934 356–363. <https://doi.org/10.1093/jpe/rtt041>

935 Newbery, D. M., & Lingenfelder, M. (2004). Resistance of a lowland rain  
936 forest to increasing drought intensity in Sabah, Borneo. *Journal of*  
937 *Tropical Ecology*, 20(6), 613–624.  
938 <https://doi.org/10.1017/S0266467404001750>

939 Oberle, B., Lee, M. R., Myers, J. A., Osazuwa-Peters, O. L., Spasojevic, M. J.,  
940 Walton, M. L., ... Zanne, A. E. (2020). Accurate forest projections  
941 require long-term wood decay experiments because plant trait effects  
942 change through time. *Global Change Biology*, 26(2), 864–875. [https://](https://doi.org/10.1111/gcb.14873)  
943 [doi.org/10.1111/gcb.14873](https://doi.org/10.1111/gcb.14873)

944 Oberle, B., Lee, M. R., Myers, J. A., Osazuwa-Peters, O. L., Spasojevic, M. J.,  
945 Walton, M. L., ... Zanne, A. E. (2019). Accurate forest projections  
946 require long-term wood decay experiments because plant trait effects  
947 change though time. *Global Change Biology*, (October), 1–12.  
948 <https://doi.org/10.1111/gcb.14873>

949 Oberst, S., Lai, J. C. S., & Evans, T. A. (2016). Termites utilise clay to build  
950 structural supports and so increase foraging resources. *Scientific*  
951 *Reports*, 6(September 2015), 1–11. <https://doi.org/10.1038/srep20990>

952 Pan, Y., Birdsey, R. a, Fang, J., Houghton, R., Kauppi, P. E., Kurz, W. a, ...  
953 Hayes, D. (2011). A large and persistent carbon sink in the world's  
954 forests. *Science*, 333(6045), 988–993.  
955 <https://doi.org/10.1126/science.1201609>

956 Pfeifer, M., Lefebvre, V., Turner, E., Cusack, J., Khoo, M. S., Chey, V. K., ...  
957 Ewers, R. M. (2015). Deadwood biomass: An underestimated carbon



958 stock in degraded tropical forests? *Environmental Research Letters*,  
959 10(4). <https://doi.org/10.1088/1748-9326/10/4/044019>

960 Pietsch, K. A., Eichenberg, D., Nadrowski, K., Bauhus, J., Buscot, F.,  
961 Purahong, W., ... Wirth, C. (2019). Wood decomposition is more  
962 strongly controlled by temperature than by tree species and  
963 decomposer diversity in highly species rich subtropical forests. *Oikos*,  
964 128(5), 701–715. <https://doi.org/10.1111/oik.04879>

965 Rice, A. H., Pyle, E. H., Saleska, S. R., Hutyra, L., Palace, M., Keller, M., ...  
966 Wofsy, S. C. (2004). Carbon balance and vegetation dynamics in an  
967 old-growth Amazonian forest. *Ecological Applications*, 14(4), 55–71.  
968 <https://doi.org/10.1890/02-6006>

969 Riutta, T., Malhi, Y., Kho, L. K., Marthews, T. R., Huaraca Huasco, W., Khoo,  
970 M. S., ... Ewers, R. M. (2018). Logging disturbance shifts net primary  
971 productivity and its allocation in Bornean tropical forests. *Global*  
972 *Change Biology*, 24(7), 2913–2928. <https://doi.org/10.1111/gcb.14068>

973 Shorohova, E., & Kapitsa, E. (2014). Influence of the substrate and  
974 ecosystem attributes on the decomposition rates of coarse woody  
975 debris in European boreal forests. *Forest Ecology and Management*,  
976 315, 173–184. <https://doi.org/10.1016/j.foreco.2013.12.025>

977 Stoklosa, A. M., Ulyshen, M. D., Fan, Z., Varner, M., Seibold, S., & Müller, J.  
978 (2016). Effects of mesh bag enclosure and termites on fine woody  
979 debris decomposition in a subtropical forest. *Basic and Applied*  
980 *Ecology*, 17(5), 463–470. <https://doi.org/10.1016/j.baae.2016.03.001>

981 Swift, M. J. (1977). The ecology of wood decomposition. *Science Progress*,  
982 64(254), 175–199. Retrieved from

983 <http://www.bcin.ca/Interface/openbcin.cgi?>  
984 [submit=submit&Chinkey=35034](http://www.bcin.ca/Interface/openbcin.cgi?submit=submit&Chinkey=35034)

985 Swinfield, T., Both, S., Riutta, T., Bongalov, B., Elias, D., Majalap-Lee, N., ...  
986 Coomes, D. (2019). Imaging spectroscopy reveals the effects of  
987 topography and logging on the leaf chemistry of tropical forest canopy  
988 trees. *Global Change Biology*, (October), 1-14. [https://doi.org/10.1111/](https://doi.org/10.1111/gcb.14903)  
989 [gcb.14903](https://doi.org/10.1111/gcb.14903)

990 Tuma, J., Fleiss, S., Eggleton, P., Frouz, J., Klimes, P., Lewis, O. T., ... Fayle,  
991 T. M. (2019). Logging of rainforest and conversion to oil palm reduces  
992 bioturbator diversity but not levels of bioturbation. *Applied Soil*  
993 *Ecology*, 144(August), 123-133.  
994 <https://doi.org/10.1016/j.apsoil.2019.07.002>

995 Ulyshen, M. D., Müller, J., & Seibold, S. (2016). Bark coverage and insects  
996 influence wood decomposition : Direct and indirect effects. *Applied*  
997 *Soil Ecology*, 105, 25-30. <https://doi.org/10.1016/j.apsoil.2016.03.017>

998 Van Wagner C.E. (1968). The Line Intersect Method in Forest Fuel  
999 Sampling. *Forest Science*, 14(1), 20-26.

1000 Warton, D. I., & Hui, F. K. C. (2011). The arcsine is asinine: the analysis of  
1001 proportions in ecology. *Ecology*, 92(1), 3-10.

1002 Yavitt, J. B., Battles, J. J., Lang, G. E., & Knight, D. H. (1995). The Canopy  
1003 Gap Regime in a Secondary Neotropical Forest in Panama. *Journal of*  
1004 *Tropical Ecology*, 11(3), 391-402.

1005 Yavitt, J. B., Wright, S. J., & Wieder, R. K. (2004). Seasonal drought and  
1006 dry-season irrigation influence leaf-litter nutrients and soil enzymes in  
1007 a moist, lowland forest in Panama. *Austral Ecology*, 29(2), 177-188.

1008 <https://doi.org/10.1111/j.1442-9993.2004.01334.x>

1009 Zanne, A. E., Lopez-Gonzalez, G., Coomes, D. A., Llic, J., Jansen, S., Lewis,  
 1010 S. L., ... Chave, J. (2009). Global wood density database. *Dryad*.

1011 Zanne, A. E., Oberle, B., Dunham, K. M., Milo, A. M., Walton, M. L., &  
 1012 Young, D. F. (2015). A deteriorating state of affairs: How endogenous  
 1013 and exogenous factors determine plant decay rates. *Journal of*  
 1014 *Ecology*, 103(6), 1421-1431. <https://doi.org/10.1111/1365-2745.12474>

1015  
 1016  
 1017  
 1018  
 1019  
 1020

1021 **Tables**

1022 **Table 1.** Mean soil temperature and moisture in closed canopy and forest  
 1023 gap sites and outputs from linear mixed effects models to assess the  
 1024 effect of gaps on soil conditions (asterisks indicate significant differences  
 1025 between closed canopy and gap sites).

Microclimate metric	Mean value		Forest		t- value	P
	Closed canopy		gap			
Min. soil temp. (°C)	7 24.0	± 0.22	5 24.4	± 0.17	2.56	0.01* 0.001
Mean soil temp. (°C)	9 25.1	± 0.07	0 25.3	± 0.07	3.22	**
Max soil temp. (°C)	3	± 0.10	8	± 0.09	1.38	0.17
Min. soil moisture	12.9	± 0.39	14.0	± 0.24	2.28	0.02*

(%)			0		6			
Mean	soil	moisture	19.5		20.9			
(%)			0	± 0.44	5	± 0.48	2.65	0.01*
Max	soil	moisture	26.7		30.2			0.001
(%)			7	± 0.58	6	± 0.76	3.37	**

1026  
1027  
1028  
1029  
1030  
1031  
1032  
1033  
1034  
1035  
1036  
1037

1038 **Table 2.** Estimates of geometric mean carbon fluxes and standard  
1039 deviation intervals (square brackets) based on 1x10<sup>6</sup> simulations for the  
1040 following scenarios: a closed canopy baseline; a scenario with 0.7% forest  
1041 gap, which, based on the LiDAR data, is the cumulative percentage of  
1042 forest area that is a gap of the same size as our focal experimental gaps  
1043 (between 0.025 and 0.16 ha); and a scenario with 2.5% forest gap, which  
1044 is the total (maximum) proportion of forest that was classified as a gap in  
1045 the LiDAR survey.

	<b>Baseline</b>	<b>0.7% gaps</b>	<b>Forest 2.5% gaps</b>	<b>Forest gaps</b>
--	-----------------	----------------------	---------------------------------	------------------------

Carbon flux (Mg C ha <sup>-1</sup> yr <sup>-1</sup> )	1.47 [0.57, 3.83]	1.56 [0.61, 3.96]	1.74 [0.70, 4.32]
Ratio to baseline	1.000	1.057 [0.969, 1.152]	1.182 [0.846, 1.477]
Carbon flux for LiDAR region (Mg C yr <sup>-1</sup> )	1380 [530, 3600]	1460 [570, 3720]	1640 [660, 4060]

1046

1047

1048 **Figure legends**

1049

1050 **Figure 1.** Schematic diagram of the study experimental design. In

1051 October 2017, we selected 10 canopy gaps (mean width 24.5 m, mean

1052 length 32 m), created by tree-fall during a storm even in July 217, and 10

1053 paired closed canopy sites (located 20 m from the edge of each gap).

1054 Within each gap and closed canopy site, we randomly placed 5 x

1055 invertebrate accessible woodblocks (represented by the grey boxes) and 5

1056 x invertebrate inaccessible woodblock (yellow boxes). Each woodblock

1057 was separated by at least 5 m and was left on the forest floor for 12-

1058 months.

1059

1060 **Figure 2.** Median plus interquartile range for mass loss from

1061 macroinvertebrate accessible (grey boxes) and macroinvertebrate

1062 inaccessible (yellow boxes) wood blocks within closed canopy and tree-fall

1063 gaps. Points are the raw data are displayed over the boxes.

1064

1065 **Figure 3.** Frequency distributions of minimum, mean and maximum soil  
1066 temperature (panels a, c, e) and soil moisture (panels b, d, f) within closed  
1067 canopy (grey ribbons) and forest gaps (yellow ribbons). Vertical dashed  
1068 lines indicate significant differences between mean microclimate  
1069 attributes in the different canopy types (closed canopy: grey lines, forest  
1070 gaps: yellow lines).

1071

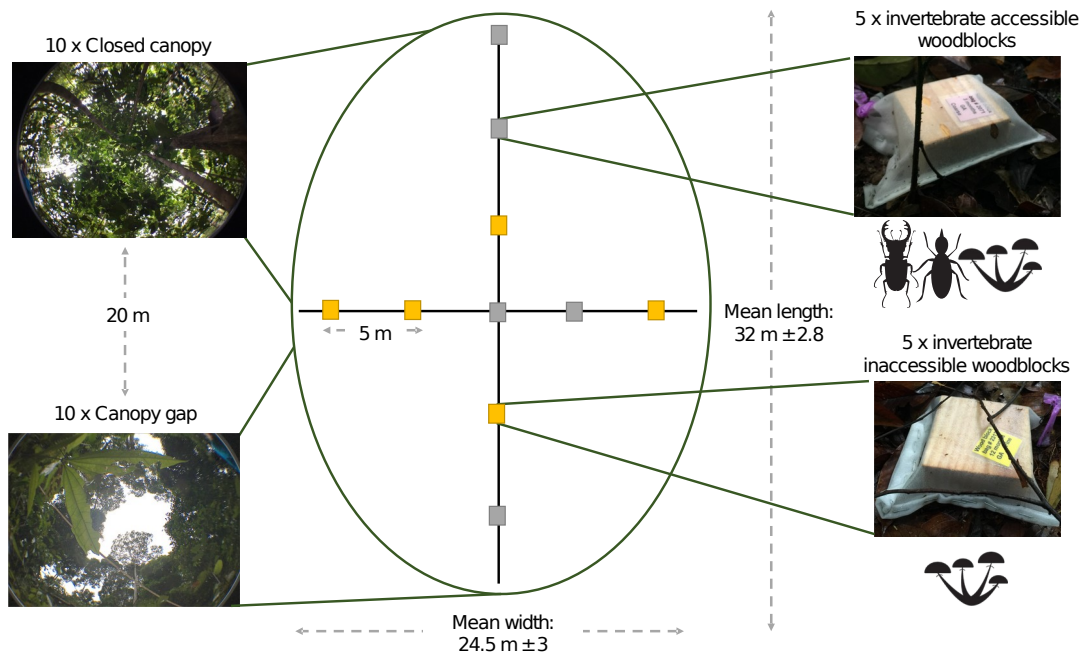
1072 **Figure 4.** Cumulative distribution of canopy gap area. Gaps of the same  
1073 area as those forming the basis of this investigation (128 gaps, between  
1074 0.025 and 0.16 ha) fall within the yellow rectangle. The total area  
1075 represented by the yellow rectangle is 6.5 ha, which is 0.7 % of the  
1076 surveyed area and represents 27% of the total gap area in the study  
1077 region. The vertical dashed line at 122 m<sup>2</sup> (0.01 ha) represents the centre  
1078 of the cumulative distribution function, where half of the gap area is  
1079 comprised of smaller gaps and the remaining half by larger gaps.

1080

1081 **Figure 5.** Median (horizontal lines) plus 95% confidence intervals  
1082 (whiskers) of the volume of deadwood on the forest floor beneath closed  
1083 canopy (grey box) and sites within 5 m of a canopy gap.

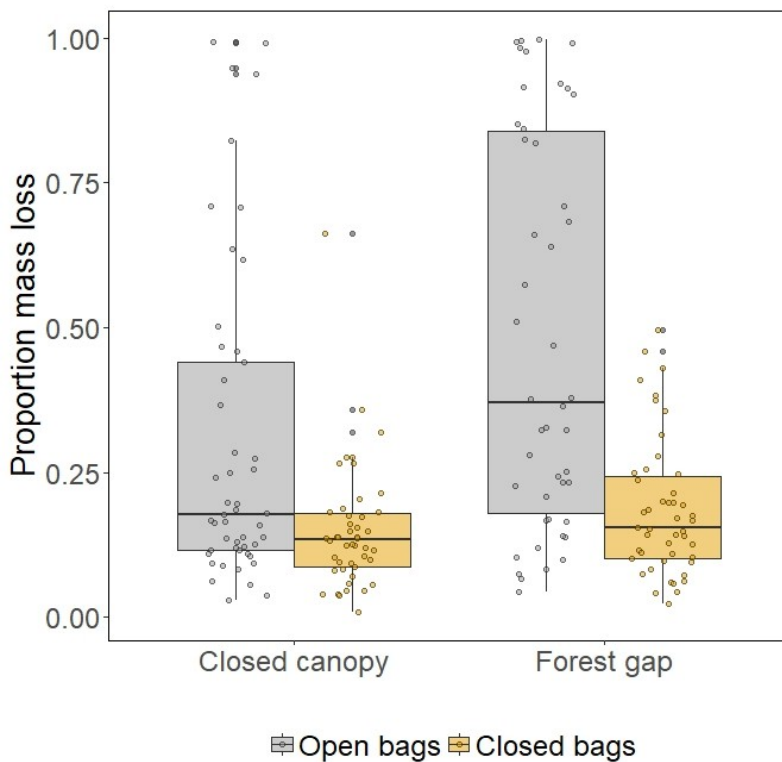
1084

1085



1086

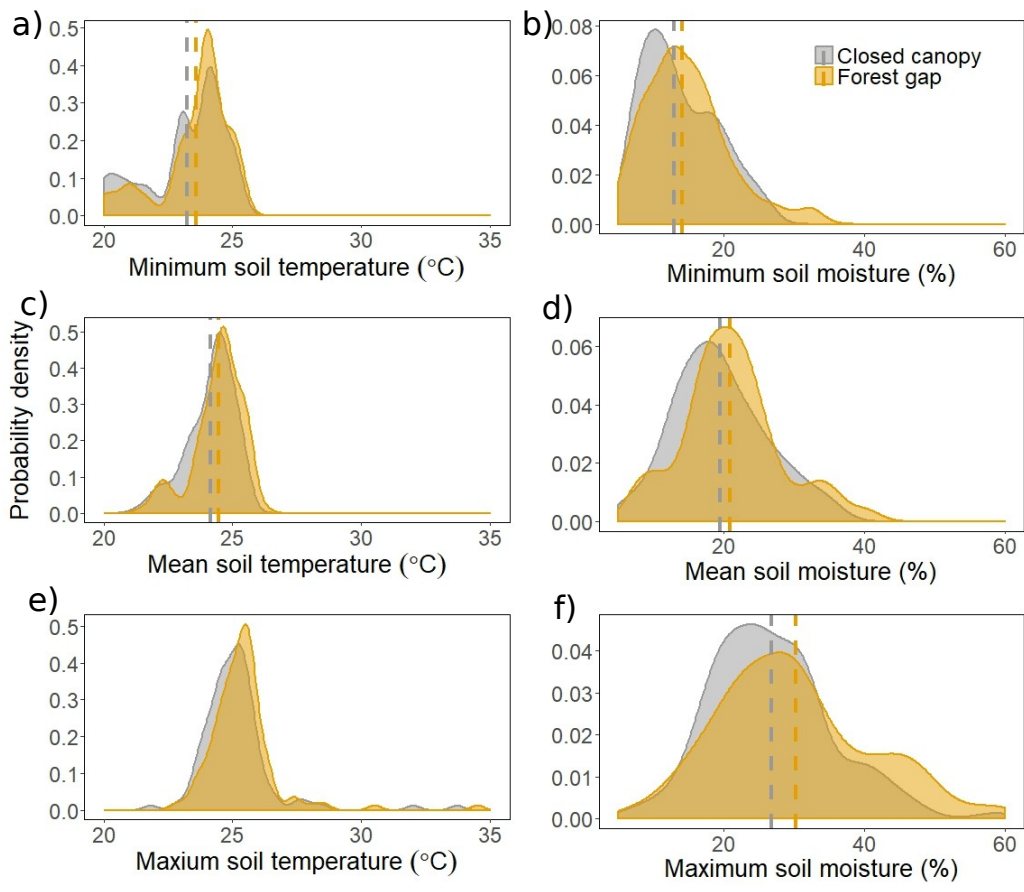
1087 **Figure 1.**



1088

1089 **Figure 2.**

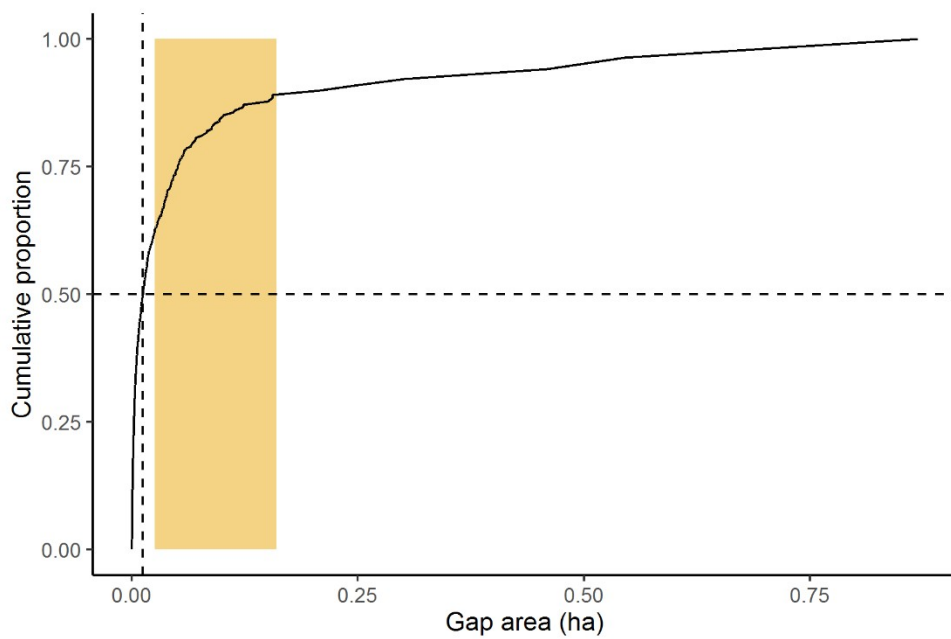
1090



1091

1092 **Figure. 3**

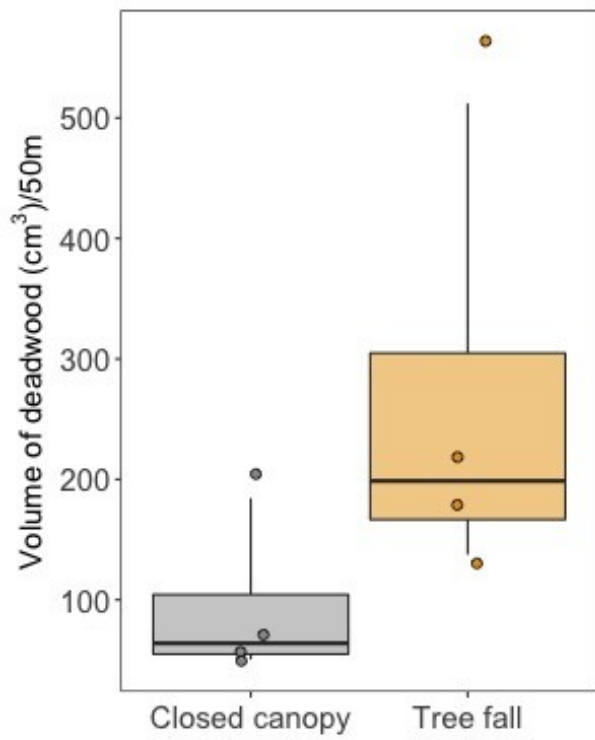
1093



1094

1095 **Figure 4.**





1096

1097 **Figure 5.**